Journal of Power Sources 196 (2011) 3149–3162

Contents lists available at ScienceDirect

Journal of Power Sources

journal homepage: www.elsevier.com/locate/jpowsour

Solid oxide fuel cell/gas turbine trigeneration system for marine applications

Lawrence Kar Chung Tse[a], Steven Wilkins[a], Niall McGlashan[a], Bernhard Urban[b], Ricardo Martinez-Botas[a,*]

[a] Department of Mechanical Engineering, Imperial College London, London SW7 2AZ, United Kingdom
[b] Fr. Lürssen Werft, Zum Alten Speicher 11, 28759 Bremen-Vegesack, Germany

ARTICLE INFO

Article history:
Received 12 August 2010
Received in revised form
19 November 2010
Accepted 20 November 2010
Available online 27 November 2010

Keywords:
Solid oxide fuel cell
Gas turbine
Trigeneration
Absorption cooling
Configuration

ABSTRACT

Shipping contributes 4.5% to global CO_2 emissions and is not covered by the Kyoto Agreement. One method of reducing CO_2 emissions on land is combined cooling heating and power (CCHP) or trigeneration, with typical combined thermal efficiencies of over 80%. Large luxury yachts are seen as an ideal entry point to the off-shore market for this developing technology considering its current high cost.

This paper investigates the feasibility of combining a SOFC-GT system and an absorption heat pump (AHP) in a trigeneration system to drive the heating ventilation and air conditioning (HVAC) and electrical base-load systems. A thermodynamic model is used to simulate the system, with various configurations and cooling loads. Measurement of actual yacht performance data forms the basis of this system simulation.

It is found that for the optimum configuration using a double effect absorption chiller in Ship 1, the net electric power increases by 47% relative to the electrical power available for a conventional SOFC-GT-HVAC system. This is due to more air cooled to a lower temperature by absorption cooling; hence less electrical cooling by the conventional HVAC unit is required. The overall efficiency is 12.1% for the conventional system, 34.9% for the system with BROAD single effect absorption chiller, 43.2% for the system with double effect absorption chiller. This shows that the overall efficiency of a trigeneration system is far higher when waste heat recovery happens.

The desiccant wheel hardly reduces moisture from the outdoor air due to a relative low mass flow rate of fuel cell exhaust available to dehumidify a very large mass flow rate of HVAC air, Hence, desiccant wheel is not recommended for this application.

1. Introduction

1.1. Shipping emissions

Shipping emissions are not covered by the Kyoto Agreement. According to the latest United Nations International Maritime Organisation report [1], shipping emitted 1.046 billion tonnes of CO_2 in the year 2007, and thereby contributed 3.3% of global CO_2 emissions. If no further actions are taken, it is concluded that shipping greenhouse gas emissions could increase by up to 250% by 2050. In addition, due to the lack of current regulations in shipping emissions, the most polluting "bunker fuels", with significantly more sulphur than road diesel, are being used as fuel, generating significant SOx emissions [2].

1.2. Harbour and sea regulations

Ships pollute when docked and left idling. According to a study by Corbett et al. [3], particulate matters from ocean-going ships cause about 60,000 deaths a year from heart and lung-related cancers, with most deaths occurring in Europe, East and South Asia near the coastlines.

As a result, new and stricter regulations are being developed for ports. In late 2007, the Los Angeles and Long Beach ports in the United States started to require ships to turn off all on-board power systems when docked, using plugged in electrical systems instead [4]. Stricter regulations regarding emissions in a wide range of sea areas are expected in the foreseeable future. Hence, it will be necessary to reduce the current level of emissions in order to be allowed to enter these restricted areas.

In Europe, particularly sensitive sea areas (PSSAs) have been designated in most parts of the sea, including the Western European Waters and the Baltic Sea areas. PSSA is defined by the International Maritime Organisation (IMO). The provisions of the United Nations Convention on the Law of the Sea (UNCLOS) are

* Corresponding author. Tel.: +44 2075947241; fax: +44 2075947023.
E-mail address: r.botas@imperial.ac.uk (R. Martinez-Botas).

0378-7753/$ – see front matter © 2010 Elsevier B.V. All rights reserved.
doi:10.1016/j.jpowsour.2010.11.099

relevant in the areas. In a PSSA, specific measures can be used to control the maritime activities in that area, such as routing measures, strict application of MARPOL (International Convention for the Prevention of Pollution from Ships) discharge and equipment requirements for ships, such as oil tankers; and installation of vessel traffic services [5].

Since August 2006, the European Union has implemented regional level regulation in the form of SOx emission control areas (SECAs), where the maximum sulphur level in marine fuels is set at 1.5%, which is one-third of the maximum level stipulated by the IMO International Convention on the Regulation of Air Pollution from Ships (MARPOL Annex VI) [6]. European SECAs include the North Sea, the Baltic Sea, and the English Channel. This means that more expensive and cleaner fuel (distillate) needs to be used. However, the Annex at this stage allows the use of marine diesel oil, as long as an approved exhaust gas cleaning system or any other verifiable technological method is fitted to a ship to reduce SOx to the required level.

Over the long term, SECAs will not be enough to reduce SOx emissions. The Marine Environment Protection Committee (MEPC) of the International Maritime Organization (IMO) amended the MARPOL Annex VI regulations in October 2008. The main changes will see the global sulphur limit to be reduced (from the current 4.5%) to 3.5% by January 2012; and progressively to 0.5% by January 2020, subject to a review to be completed by 2018.

In July 2010, the sulphur limit at SECAs was reduced to 1.0%; with further reduction to 0.1% from January 2015.

Further, in January 2010, a maximum 0.1% sulphur limit was in place for inland waterway vessels and ships at berth in all European Community Ports. The alternative will be to use approved exhaust gas cleaning system and/or use shore side power supplies.

Besides SOx emissions, NOx emissions levels regulation has been revised and tightened as of October 2008. The new regulation follows a 3-tier approach. Tier I applies to diesel engines installed in ships built between January 2000 and January 2011. Tier II applies to new ships built on and after January 2011. Tier III applies to new ships built on and after January 2016, operating at Emissions Control Areas. The emissions limits in each tier vary with the engine revolutions per minute (rpm).

Should an upgrade kit be available, NOx standards will retroactively apply to existing ships built from 1990 to 2000 with engines >5000 kW and $\geq$90 l displacement [6].

Moreover, incorporating shipping into a global carbon dioxide emissions trading scheme or charging a climate levy on bunker fuel are efficient and cost effective in delivering emissions reductions, and likely to be introduced in the 2012 post-Kyoto climate regime [1].

In addition, the Shipping Emissions Abatement and Trading (SEAaT) has carried out a Sulphur Emissions Offsetting Pilot Project, to explore the application of emissions trading for reducing sulphur emissions from shipping activities [7].

Due to the increasing regulations, ship owners are encouraged to seek ways to increase energy efficiency and reduce consumption of fuels onboard.

1.3. Marine fuel cell-gas turbine system

The most common power source on board of luxury yachts as well as other seagoing vessels is the diesel generator. The diesel generator has a good ratio of available power to mass and volume.

The demand for available power is steadily increasing and ever larger engines with high power outputs are being installed. However, diesel engines produce noise and vibrations as well as emissions such as NOx, SOx and particulates. In order to minimise noise and vibrations, shock absorbers and other passive means are used to reduce the propagation of noise and vibrations within the vessel. These passive provisions are cost intense and additional weight is added to the ship.

In order to reduce fuel consumption and emissions, one option is to replace some of the existing diesel generators with a solid oxide fuel cell (SOFC). The noise and vibration level on board can also be reduced significantly.

The power demand of a yacht depends on its mode of operation. Most electrical power is required when the electrically powered auxiliary drives, like stern and bow thrusters or pump jets, are used. These drives are used in manoeuvring or dynamic positioning mode. The modes of operation are not bounded to any fixed schedule but depend on the habits of the owner.

Due to the relatively new technology of the fuel cell, the long start-up and stopping time (typically 18–30 h on average) and limited load following capability, fuel cells are only operated at constant power output to meet base load demands. This means that the fuel cell system is only an auxiliary power unit (APU).

The minimum average load occurs in harbour operation. The base load of a mega yacht is in the range of 15–25% of total installed electrical power. Small load fluctuations will be compensated by an energy storage system or a gas turbine system. Additional load during the sea mode and manoeuvre mode can be provided by the conventional diesel generators, operating in parallel to a fuel cell system [5].

Past papers have only discussed the application of a 300 W proton exchange membrane fuel cell with reforming for sailing yacht application [8]; and a 500 kWe Molten carbonate fuel cell system with diesel reforming for cruise, passenger or commercial ship [9].

1.4. Choice of fuel for marine SOFC-GT systems

The choice of fuel for the powering of a fuel cell system onboard the yacht depends on the available technologies for fuel cells and the fuel production pathways, limited by the restriction of fuel and fuel quality for shipping.

The following shows the pros and cons of fuel available from each production pathway; and the safety and requirements as a fuel for a fuel cell system.

1.4.1. Hydrogen

Although hydrogen itself is a compatible fuel with the majority of fuel cell systems, it is impractical to use as a primary shipping fuel, due to:

- Relative low power density (i.e., large volume requirements)
- Lack of supply infrastructure
- Only relevant for applications with low power and frequent refuelling opportunities (i.e., ferries, inland water vessels, coastal vessels) [39].

1.4.2. Liquid hydrocarbons

In general liquid hydrocarbons have significant advantages over hydrogen for energy storage onboard the yacht, namely:

- Relative high power density
- Supply infrastructure is available (at least for marine diesel oil or marine gas oil) or possible with "moderate" investments being established
- Relevant for high power applications without frequent refuelling opportunities (i.e., all other seagoing ships) [39].

1.4.3. Diesel

The use of shipping diesel is the preferred option given the existing infrastructure of many shipyards. Yacht owners would usually try to run the engines with high quality fuel. These fuels have a sulphur content of approximately 0.2–0.5%, which significantly hinders reformation to methane or hydrogen for use in the fuel cell. Indeed, the technological feasibility and cost for reformers which can deal with such high sulphur content rules out diesel as an option for shipping [5].

A possible option would be to have a separate fuel tank for sulphur-free diesel which is processed on-shore especially for fuel cell yachts. Reformation of sulphur-free diesel is possible and has been demonstrated in research projects. This would generate additional costs in the production of such fuel, but the components and the procedure to design such a system are well known and it implies minimum risks for the shipyard and the owner [5].

1.4.4. Liquefied petroleum gas (LPG)

Liquefied petroleum gas (LPG) needs to be stored in cylindrical pressure tanks at approximately 8 bar, and has to be placed in a separate room with additional safety equipment. Compared to a diesel tank, less fuel can be stored within a given space.

LPG is available worldwide and present infrastructures can be used to supply yacht marinas. Reformation of LPG is necessary in order to receive a methane rich gas that is suitable for the SOFC [5].

1.4.5. Liquefied natural gas

Liquefied natural gas (LNG) is a natural gas (primarily methane, CH_4) that has been converted to liquid form for ease of storage or transport. A reliable infrastructure for LNG is currently not available for shipping, and is therefore not a current option. Indeed for ships/yachts that are frequently at many ports rather than those with defined routes, the access to LNG is far more critical.

1.4.6. Fuel safety and requirements

The International Maritime Organisation (IMO) strictly regulates the use of permissible fuels for waterborne applications. In general only fuels with a flash point above 60 °C are permitted. Fuels with a lower flash point require special measures regarding fuel handling, storage and safety devices [5].

A fuel for a SOFC needs to be able to be reformed to form a methane rich gas. This gas must be free of any components that lead to fast degradation of the stack. The land based system is designed to be fed by natural gas. Minimum change to the SOFC must be made if LNG is used on board. In the past years LNG has gained more and more importance as a fossil fuel. Many LNG terminals have been built or are being planned. Also several ferries have been built in Norway which are fuelled with LNG [5].

1.4.7. Candidate fuels for fuel cell systems

Based on the fuel availability, practicality and safety criteria, the following conclusions are made for a candidate fuel for fuel cell systems:

- LPG is the most compatible fuel for near to mid-term
- Diesel is preferred for long-term
  - Reforming and desulphurisation remains too challenging
  - Synthetic (zero sulphur) diesels can be made from *Fischer–Tropsch* process, but not currently available
- When LNG becomes more widely available, it will also be a long-term option.

1.5. Trigeneration

Trigeneration, also known as combined heating, cooling and power (CCHP), is a way of making the best use of the chemical energy of the fuel to generate electricity, with the heat from the exhaust being utilised by providing heating. At the same time, cooling can be produced from absorption or desiccant cooling, therefore reduce the consumption of electricity in a conventional air conditioning unit. Hence, the overall efficiency can be increased to close to 90%.

No known paper has been written concerning the application of a solid oxide fuel cell-gas turbine-trigeneration system for marine applications, although a number of papers have written about FC-GT-trigeneration systems for a residential district trigeneration plant [10], for an office [11] and for a hospital [12]. Conventional trigeneration systems can be found in various stationary applications such as; industrial processes [13], individual households in remote areas [14], an office building [15], a hotel [16], a hospital [17] and at an airport [18,19]. The heat source for absorption or desiccant heating/cooling is commonly from solar [20] and exhaust heat streams from industrial processes or other power generation cycles [21].

In this paper, a number of novel SOFC-GT trigeneration systems are considered and compared with conventional heating ventilation and air conditioning (HVAC) systems, to determine the potential for energy savings by absorption and desiccant devices in providing cooling.

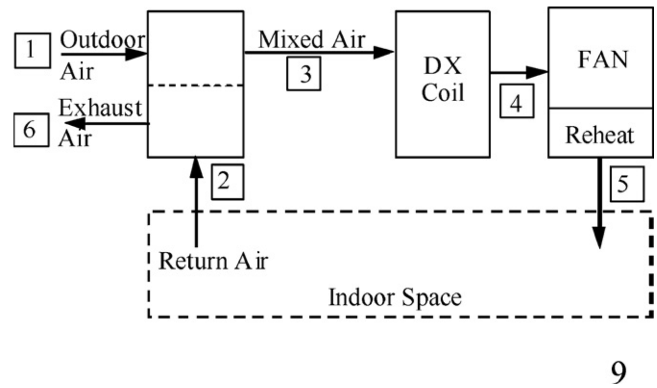

Fig. 1. Schematic diagram for the conventional HVAC system.

2. Hybrid cycles considered

A SOFC-GT/conventional HVAC system is compared with novel systems consisting of a combination of absorption chiller, desiccant wheel and conventional HVAC system. The following system configurations are considered.

2.1. SOFC-GT + conventional HVAC

The SOFC-GT system and conventional HVAC system run independently of each other. The SOFC-GT system supplies electricity to run the air conditioning unit and fan (Fig. 1).

2.2. SOFC-GT + absorption chiller + HVAC

In this configuration, the absorption chiller provides cooling for the mixed air via the CHP coil (between stations 3 and 4), but not enough for the air to reach the required absolute humidity. Hence, a conventional direct expansion (DX) coil is used to cool the air further to condense water at saturation (Fig. 2).

2.3. SOFC-GT + desiccant wheel + HVAC

This configuration uses a desiccant wheel to dry mixed air to reach the required absolute humidity. The air temperature

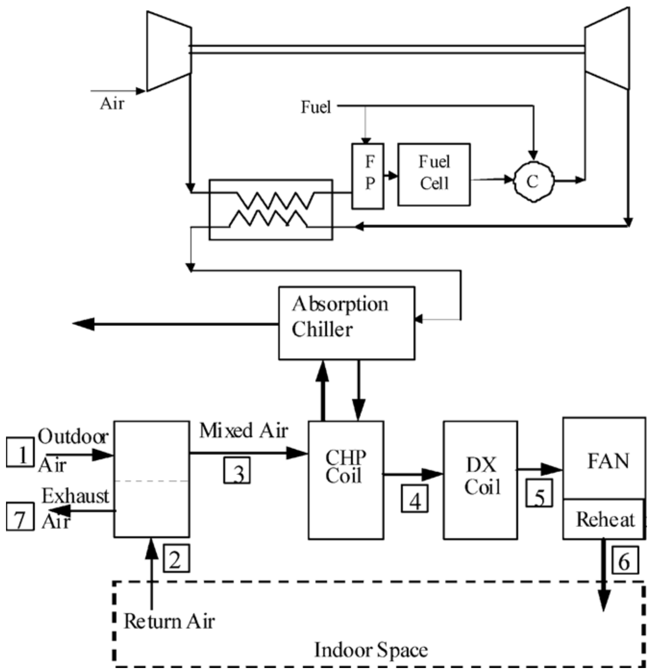

Fig. 2. Schematic diagram for the SOFC-GT-absorption chiller-HVAC system.

is increased, and therefore needs to be cooled down, which is achieved using a direct expansion (DX) coil (Fig. 3).

2.4. SOFC-GT + absorption chiller + desiccant wheel + HVAC

This configuration is similar to the previous one. The only advantage is that air cooling after the desiccant wheel is partly achieved by using chilled water from the absorption chiller entering the CHP Coil. Any additional cooling required is supplied by the conventional direct expansion (DX) coil (Fig. 4).

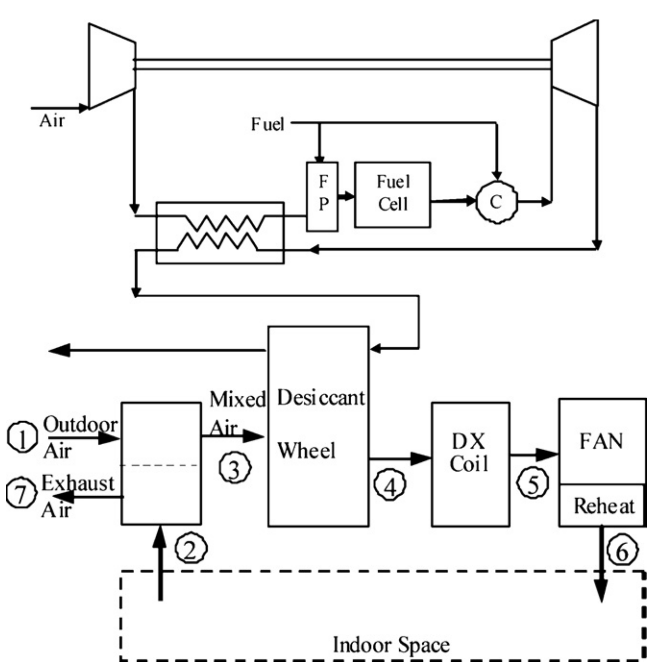

Fig. 3. Schematic diagram for the SOFC-GT-desiccant wheel-HVAC system.

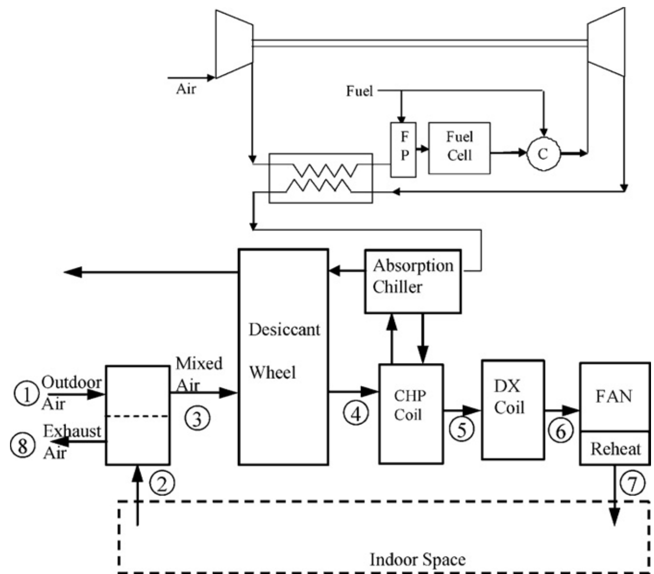

Fig. 4. Schematic diagram for the SOFC-GT-absorption chiller-desiccant wheel-HVAC system.

3. Thermodynamic modelling

3.1. SOFC-GT

The recuperated hybrid SOFC-GT system stabilises SOFC operation and increases thermal efficiency [22]. The recuperated hybrid cycle diagram and station numbers are shown in Fig. 5.

Based on the Imperial College London system configuration modelling results in [22–25], the following steady-state design point conditions are chosen for the hybrid cycle, by optimising specific power output and system thermal efficiency:

- Pressure ratio = 4
- Turbine inlet temperature = 1250 K
- Fuel cell current density = 300 mA cm^{-2}.

A SOFC-GT model was formulated on the conservation of mass and energy at equilibrium. The model incorporates the Siemens-Westinghouse fuel cell design which utilises the fuel cell stack heat to both aid the internal reforming process and to preheat the incoming air, as well as anodic recirculation [22].

The system modelled was a SOFC-GT sub-system, with variable geometry compressor and turbine stages to maintain acceptable surge-margins (compressor inlet guide vanes and diffuser vanes, and turbine nozzle inlet guide vanes). The compressor/turbine maps are based on a design point of 0.31/0.32 kg s^{-1} and 4:1/1:3.4

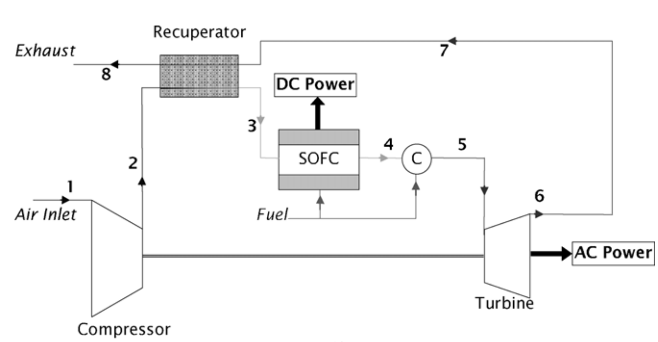

Fig. 5. Schematic diagram of the recuperated SOFC-GT cycle [22].

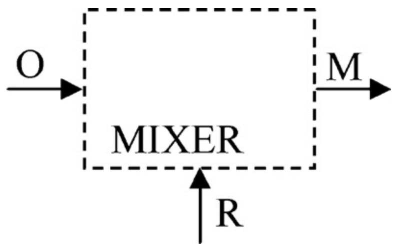

Fig. 6. Control volume of the mixer.

pressure ratio, developed by National Technical University of Athens [26]. The external combustor is used for start-up and to maintain a suitable turbine inlet temperature (TIT).

The fuel cell operates at 1000 °C, and total power density from the SOFC-GT system (after taking into account of parasitic power) is 602.5 kJ kg^{-1}. Methane is supplied as fuel and internal reforming occurs within the fuel cell system. For a 250 kW SOFC-GT system, the air flow rate into the fuel cell is 0.415 kg s^{-1}. When fuel flow is taken into account, the total flow rate of the exhaust stream from the SOFC-GT is 0.423 kg s^{-1}.

The scope of the paper only covers the fuel entering into the SOFC system. As shown in the earlier section, LPG is the most likely near-term choice of fuel, with LNG and diesel as long-term fuel choices. All the fuels can be reformed to methane before feeding into the fuel cell system for internal reforming.

3.2. HVAC system [roof top unit (RTU)]

A schematic diagram of a conventional electrically driven vapour compression HVAC system or roof top unit (RTU) can be found in Fig. 1. In operation, the outdoor air [station 1] mixes with return air [station 2] in the ratio of 1:4. The mixed air [station 3] is then cooled down by the direct expansion (DX) coil. In the DX coil, the air is cooled until it reaches 100% humidity. Water condenses with the temperature dropping until it reaches the required absolute humidity [station 4]. The reheating warms the air back to the required air temperature. The cooled and dried air then enters the indoor space [station 5]. A fan is required to increases the pressure of the air and promote air flow.

Cengel and Boles [27] shows that the coefficient of performance (COP) of a typical HVAC unit is 2.3–3.5. Nayak et al. [28] tested a real HVAC unit in a building with a COP value of 3.5. Hence, COP = 3.5 is chosen for the DX coil in the conventional HVAC unit for the model described in this paper.

3.2.1. Control volume equations

The system can be split into a number of control volumes, with mass continuity equations (MCE) and steady flow energy equations (SFEE) to be solved (Figs. 6–9).

3.2.1.1. HVAC mixer. See Fig. 6.

MCE:

$$\dot{m}_{aOA} + \dot{m}_{aRA} + \dot{m}_{vOA} + \dot{m}_{vRA} = \dot{m}_{aMA} + \dot{m}_{vMA} \quad (1)$$

where $\dot{m}_{aOA}, \dot{m}_{aRA}, \dot{m}_{vOA}, \dot{m}_{vRA}, \dot{m}_{aMA}, \dot{m}_{vMA}$ are respectively the mass flow rates of air component in outdoor air, air component in re-circulated air, water vapour component in outdoor air, water vapour component in re-circulated air, dry air component in mixed air, water vapour component in mixed air.

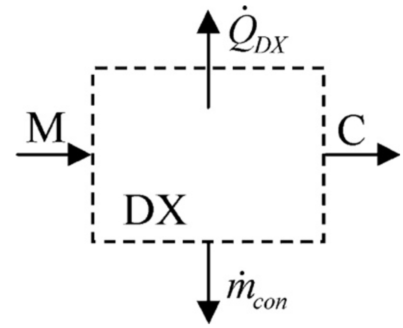

Fig. 7. Control volume of the direct expansion coil.

SFEE:

$$\dot{m}_{aMA}h_{MA} = \dot{m}_{aOA}h_{OA} + \dot{m}_{aRA}h_{RA} \quad (2)$$

where h_{MA}, h_{OA}, h_{RA} are respectively enthalpies of the mixed air, outdoor air and re-circulated air.

3.2.1.2. Direct expansion coil (DX). See Fig. 7.

MCE:

$$\dot{m}_{aMA} + \dot{m}_{vMA} = \dot{m}_{con} + \dot{m}_{aCA} + \dot{m}_{vCA} \quad (3)$$

where $\dot{m}_{aMA}$, $\dot{m}_{vMA}$, $\dot{m}_{con}$, $\dot{m}_{aCA}$ and $\dot{m}_{vCA}$ are respectively the mass flow rates of dry air component in mixed air, water vapour component in mixed air, condensate, dry air component in cooled air and water vapour component in cooled air.

SFEE:

$$-\left|\dot{Q}_{DX}\right| = \dot{m}_{con}h_{con} + \dot{m}_{aCA}h_{CA} - \dot{m}_{aMA}h_{MA} \quad (4)$$

where $\dot{Q}_{DX}$ is the heat power removed by the direct expansion coil; h_{CA} is the enthalpy of the cooled air; h_{MA} is the enthalpy of the mixed air; h_{con} is the enthalpy of condensation based on $T_{CA.}$

T_{CA} is the cooled air temperature after the cooling and dehumidification processes, in order to reach the relative humidity level required by the ship indoor environment, before the reheating process. It is at 1 atmospheric pressure, obtained from the subcooled liquid steam tables. Note that the sensible heat is taken into consideration in the steady flow energy equation (Eq. (4)).

3.2.1.3. Fan and (variable air valve with) reheater (RH). See Fig. 8.

MCE:

$$\dot{m}_{aCA} + \dot{m}_{vCA} = \dot{m}_{aSA} + \dot{m}_{vSA} \quad (5)$$

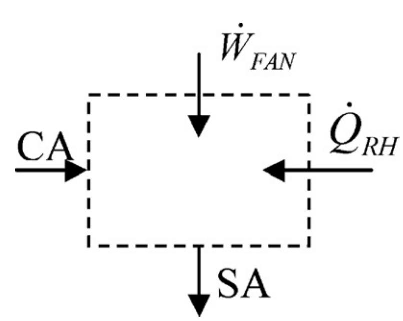

Fig. 8. Control volume of the fan and variable air valve with reheater.

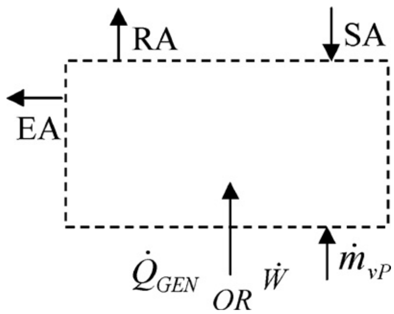

Fig. 9. Control volume of the room.

where $\dot{m}_{aSA}$ and $\dot{m}_{vSA}$ are respectively the mass flow rates of dry air component in supply air for the room, water vapour component in supply air for the room.

SFEE:

$$\left|\dot{Q}_{RH}\right| + \left|\dot{W}_{FAN}\right| = \dot{m}_{aSA}h_{SA} - \dot{m}_{aCA}h_{CA} \quad (6)$$

where $\dot{Q}_{RH}$, $\dot{W}_{FAN}$, h_{SA} and h_{CA} are respectively the heat power from the reheater, work power by the fan, enthalpy of the supply air and enthalpy of the cooled air.

3.2.1.4. Room. See Fig. 9.

MCE:

$$\dot{m}_{aSA} + \dot{m}_{vSA} + \dot{m}_{vP} = \dot{m}_{aEA} + \dot{m}_{vEA} + \dot{m}_{aRA} + \dot{m}_{vRA} \quad (7)$$

where $\dot{m}_{aSA}$, $\dot{m}_{vSA}$, $\dot{m}_{vP}$, $\dot{m}_{aEA}$, $\dot{m}_{vEA}$, $\dot{m}_{aRA}$, $\dot{m}_{vRA}$ are respectively the mass flow rates of dry air component in supply air, water vapour component in supply air, water vapour from the sweat of people inside the room, dry air component in exhaust air, water vapour component in exhaust air, dry air component in re-circulated air, water vapour component in re-circulated air.

SFEE:

$$\left|\dot{Q}_{GEN}\right| = \dot{m}_{aEA}h_{EA} + \dot{m}_{aRA}h_{RA} - \dot{m}_{vP}h_{vP} - \dot{m}_{aSA}h_{SA} \quad (8)$$

where h_{EA}, h_{RA}, h_{vP}, h_{SA} are respectively the enthalpies of the exhaust air, re-circulated air, water vapour from sweat of people inside the room, supply air; $|\dot{Q}_{GEN}|$ is the net total heat power generated by people at indoor and the net electric power usage (this could be considered as $\dot{W}$).

3.3. Absorption chiller

An absorption chiller is a device that uses heat energy for cooling instead of a mechanical compressor that consumes electrical energy. A schematic diagram of a standard single stage chiller system is shown as part of Fig. 10. Waste heat from the SOFC-GT system exhaust stream is used to drive the chiller; heat is transferred to the generator (Q_{gen}) and used to produce chilled water to cool air at the CHP coil of the HVAC (Q_L).

Assumptions: Ideal heat transfer between working fluids, no external heat losses.

A number of different chiller configurations are considered in this paper. These configurations are presented below:

Single effect absorption chillers

- NH_3–H_2O system requires:
  - Generator temperature in 125–170 °C range with air-cooled absorber and 80–120 °C with water-cooled absorber.
  - COP: 0.6–0.7.
- LiBr–H_2O system requires:
  - Water to be used as coolant in the absorber and condenser to avoid LiBr coolant crystallization. However, Liao et al. [29] shows that air can be used as coolant while avoiding crystallization, by chilled water temperature control and exhaust temperature control.
  - Has a COP higher than the NH_3–H_2O system.
  - COP: 0.6–0.8.
  - *Disadvantage:* evaporator is unable to operate at temperatures much below 2 °C since the refrigerant is water vapour.
- Single effect absorption chiller mainly used for building cooling load, where chilled water is required at 6–7 °C; and can operate with hot water temperature ranging from about 80 to 150 °C when water is pressurised.

Double effect absorption chillers

- Have two stages of generation to separate the refrigerant from the absorbent.
- Temperature range of the heat source needed to drive the high-stage generator: 155–205 °C.
- COP: approximately 0.9–1.2.

Triple effect absorption chillers

- COP = 1.3–1.7 [31].

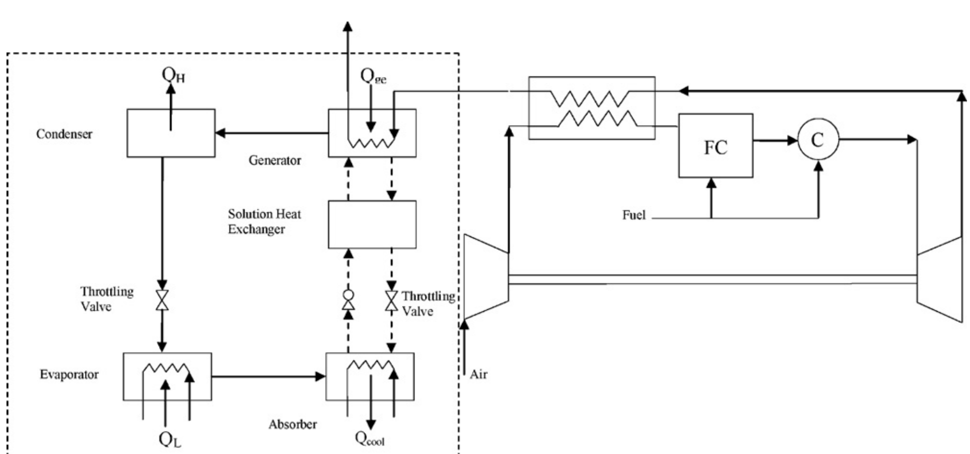

Fig. 10. Schematic diagram for absorption chiller (dotted) linked to the SOFC-GT system.

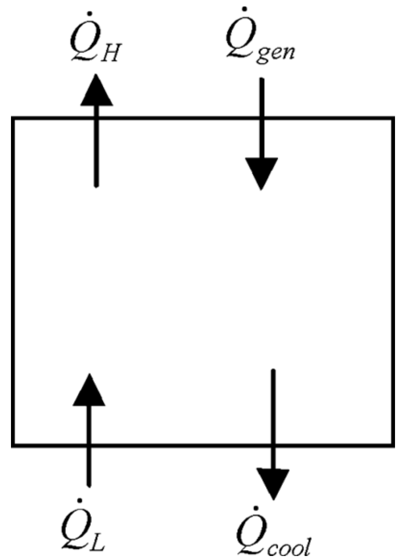

Fig. 11. Control volume of the absorption chiller.

- *Advantages:* Higher COP compared with single and double effect absorption chiller. A higher temperature heat source can be used [40].
- *Disadvantages:* Operating pressure and temperature are higher compared with single and double effect absorption chiller. More expensive material is required for pressure vessels and to prevent corrosion due to lithium bromide coolant at higher temperature. Also, with more condensers and absorbers, the system is more complex and has higher maintenance cost [40].

3.3.1. Control volume equations

See Fig. 11.

MCE:

None.

SFEE:

$$\dot{Q}_H + \dot{Q}_{cool} = \dot{Q}_{gen} + \dot{Q}_L \quad (9)$$

where $\dot{Q}_H$, $\dot{Q}_{cool}$, $\dot{Q}_{gen}$, $\dot{Q}_L$ are respectively the heat power of the condenser, absorber, generator (heat source), evaporator.

Others:

$$COP = \frac{\dot{Q}_L}{\dot{Q}_{gen} + \dot{W}_{pump,in}} \approx \frac{\dot{Q}_L}{\dot{Q}_{gen}} < 1 \quad (10)$$

$$COP_{rev,absorption} = \frac{\dot{Q}_L}{\dot{Q}_{gen}} = \eta_{th,rev} COP_{R,rev} = \left(1 - \frac{T_0}{T_s}\right)\left(\frac{T_L}{T_0 - T_L}\right) \quad (11)$$

where $\dot{W}_{pump,in}$ is the pump power input; T_L, T_0, and T_s are respectively the temperature of the refrigerated space, the environment and the heat source; $\eta_{th,rev}$ is the reversible thermal efficiency of the refrigeration system; $COP_{rev,absorption}$ is the overall COP of an absorption refrigeration system under reversible conditions.

$$\dot{W} = \eta_{th,rev}\dot{Q}_{gen} = \left(1 - \frac{T_0}{T_s}\right)\dot{Q}_{gen} \quad \text{and} \quad \dot{Q}_L = COP_{R,rev}\dot{W} = \left(\frac{T_L}{T_0 - T_L}\right)\dot{W} \quad (12)$$

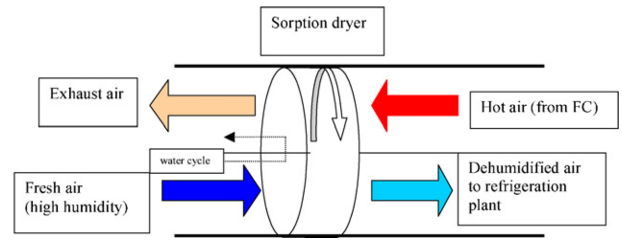

Fig. 12. Principle of desiccant wheel [38].

Where $\dot{W}$ is the work output of the heat engine supplied to the Carnot refrigerator to remove heat from the refrigerated space.

3.4. Desiccant wheel

A desiccant wheel contains silica gel to adsorb moisture from fresh outdoor air. The dehumidified and warmed air is then entered into a refrigeration plant for cooling.

The wheel is then rotated to the other side where heat from the hot stream from the fuel cell system (i.e., post-recuperator), is used to warm up the silica gel, releasing the water in to the exhaust stream. The silica gel is reactivated by this means (Fig. 12).

One example of a desiccant wheel is manufactured by NovelAire Technologies: It allows high temperature media for use with maximum regenerating temperature of 350 °F (176.7 °C). Two types of desiccant are available:

- *Silica gel:* It is used when inlet relative humidity is high (>60%), and when efficient removal of moisture is required.
- *Molecular sieve:* It is used when inlet relative humidity is low (<50%), and when low dew points are required.

The regeneration area for dehumidifying moisture normally takes up a quarter (with the maximum of half) of the total desiccant wheel area, while the mixed stream will go passed the rest of the area [32].

In this application, the silica gel model is applied. Also, the volumetric flow rate of the fuel cell exhaust stream must match the HVAC flow rate. Due to relative low flow rate of the fuel cell hybrid system exhaust stream compared to the HVAC flow rate, the only way to make it work is to choose 3 HVAC units for the ship (less than the typical 7 HVAC units), with 1/11 of the wheel area for the dehumidification of outdoor air and 10/11 for the reactivation of silica gel.

An alternative, novel one-rotor, two-stage rotary desiccant cooling system is described in Ge et al. [33].

The advantage of desiccant wheel is that it is reasonably compact (takes up significantly less space) and will fit well into a ship with limited space. It is lighter and simpler compared to an absorption chiller [37]. However, the fact that it has moving parts means that this needs to be maintained. It has less liquid compared to an absorption chiller.

A desiccant wheel increases the temperature of the outdoor air after dehumification via regeneration. To reduce the temperature, the air is passed through a heat exchanger [33] or an enthalpy wheel [34], and afterwards evaporative coolers [35] or vapour compression refrigeration chillers [36] to remove the heat. An enthalpy wheel is similar to a desiccant wheel but without the silica gel to absorb moisture, and acts more like a heat exchanger.

In terms of thermal management, the desiccant wheel has the advantage of utilising extra heat from the exhaust for dehumidifying the humid outdoor air [37]. However, the downside is that extra energy is needed to cool down the mixed air. The reduction in net electric power available for base load exceeds the gain in overall system efficiency.

Fig. 13. Control volume of the desiccant wheel.

3.4.1. Control volume equations

Assumption: Adiabatic heat transfer [constant enthalpy process] (Fig. 13).

See Fig. 13.

Assumption: Adiabatic heat transfer [constant enthalpy process].

MCE:

$$\dot{m}_{aB1} + \dot{m}_{fB1} + \dot{m}_{aT2} + \dot{m}_{fT2} = \dot{m}_{aB2} + \dot{m}_{fB2} + \dot{m}_{aT1} + \dot{m}_{fT1} \quad (13)$$

where $\dot{m}_{aB1}, \dot{m}_{fB1}, \dot{m}_{aT2}, \dot{m}_{fT2}, \dot{m}_{aB2}, \dot{m}_{fB2}, \dot{m}_{aT1}, \dot{m}_{fT1}$ are respectively the mass flow rates of air component of fresh air, water vapour component of fresh air, air component of hot air from fuel cell, water vapour component of hot air from fuel cell, air component of dehumidified air, water vapour component of dehumidified air, air component of humidified exhaust air, water vapour component of humidified exhaust air.

SFEE:

$$\dot{m}_{aB1}h_{aB1} + \dot{m}_{fB1}h_{fB1} + \dot{m}_{aT2}h_{aT2} + \dot{m}_{fT2}h_{fT2} = \dot{m}_{aB2}h_{aB2} + \dot{m}_{fB2}h_{fB2} + \dot{m}_{aT1}h_{aT1} + \dot{m}_{fT1}h_{fT1} \quad (14)$$

where $h_{aB1}, h_{fB1}, h_{aT2}, h_{fT2}, h_{aB2}, h_{fB2}, h_{aT1}, h_{fT1}$ are respectively the enthalpies of air component of fresh air, water vapour component of fresh air, air component of hot air from fuel cell, water vapour component of hot air from fuel cell, air component of dehumidified air, water vapour component of dehumidified air, air component of humidified exhaust air, water vapour component of humidified exhaust air.

3.5. Power split between diesel engine and SOFC-GT hybrid system

It is mentioned earlier that the SOFC-GT hybrid system is an APU. In this model, it is assumed that the based load is at 250 kW and is total provided by the APU. This accounts for a quarter of the total peak power required by the ship. The rest of the 750 kW energy (mainly for propulsion) is supplied by the conventional diesel engine. The peak energy for the ship is 1 MW.

4. Computational implementation

The HVAC calculations are done by solving mass continuity and the steady flow energy equations with the help of the psychometric diagrams calculation software: *Get Psyched*.

The absorption chiller calculations are based on the Saito et al. [11] model for determining the amount of cooling that the absorption chiller can provide, relative to the electric power that the SOFC-GT system that can provide. To verify the calculation, the single effect exhaust absorption chiller performance data provided by the Chinese manufacturer BROAD [30] are used to simulate the cooling available.

For sizing purposes, the desiccant wheel calculations are performed using a simulation software provided by the desiccant wheel manufacturer, NovelAire Technologies.

The efficiency calculation for each scenario is dependent on the components. The equation for cases with desiccant wheel and exhaust gas driven double effect absorption heat pump are based on modified efficiency equations found in [28,38].

The overall system efficiency is:

$$\eta_{CHP} = \frac{\textit{Net electric power} + \textit{Total waste heat utilised}}{\textit{Methane fuel input}} \quad (15)$$

where *Net electric power* is the amount of electrical power available to the ship after taking into account of power required to operate the HVAC unit; fan and reheater; absorption chiller, and/or desiccant wheel. *Total waste heat utilised* is the amount of waste heat from the SOFC-GT system exhaust utilised in an absorption chiller and/or a desiccant wheel within the system.

5. Results and discussion

5.1. Ship scenarios

A typical Lürssen ship is designed to operate smoothly at a relative humidity of 70% at a temperature of 35 °C, with the worst case scenario of 100% relative humidity and a temperature of 45 °C. The indoor environment is modelled to be with less demanding humidity, therefore the dew point temperature at which the required absolute humidity is reached will not be too low. Hence, the reheating energy required to increase to 20 °C is minor, compared to the electric cooling and dehumidifying. Data from two additional real life Lürssen ships are available to compare and contrast the performance results. The indoor and outdoor conditions of the three scenarios are summarised in Table 1.

It is also assumed that for a SOFC-GT system producing 250 kW electric power, any electrical energy left after HVAC cooling, reheating is used for electrical appliances and lighting. The same amount of energy will eventually become heat, which needs to be removed from the indoor environment. Due to the difference in temperature and humidity between the indoor and outdoor environments, calculations from mass continuity and steady flow energy equations shows that heat exceeding 250 kW needs to be removed for the SOFC-GT-conventional HVAC system. If a desiccant wheel is in the air conditioning system, more heat will be produced, further increasing the heat load of the system.

5.2. System configurations

As an example, a yacht with 7 air conditioning units manufactured by the company ALKO-THERM is used. Each unit has an air volumetric flow rate of 6419 $m^3 h^{-1}$. The mixed air consists of 80% return air and 20% outdoor air. For each ship, it is possible to use a combination of conventional a HVAC unit and/or (single or double) absorption chiller. In each case, the psychometric diagram will be different. To explain how the psychometric chart varies in different cases, Ship 1 is chosen as a realistic example in the psychometric diagrams shown in the coming sub-sections.

Table 1
Indoor and outside conditions of 3 ships.

	Worst case	Ship 1	Ship 2
Outdoor humidity (%)	100	70	85
Outdoor temp. (°C)	45	38	35
Sea temp. (°C)	41	34	32
Indoor humidity (%)	80	50	55
Indoor temp. (°C)	20	21	21

5.2.1. SOFC-GT + conventional HVAC

The shape of the graph of the psychometric diagram of the air conditioning process is very similar to that of the case with absorption chiller. The difference is that there is no station 4, which represents that point at which the temperature of the mixed air is reduced to, after being cooled down by the absorption cooler. The required indoor conditions are shown at station 6. In order to reach these conditions, mixed air at station 3 must be cooled down until it reaches 100% saturation curve (the leftmost curve). Condensation starts to occur and the temperature keeps dropping until the required absolute humidity is reached (at station 5). The air is then heated up by a heater to reach the target conditions.

5.2.2. SOFC-GT + absorption chiller + HVAC

According to Saito et al. [11], a 30 kW SOFC-GT system (26.2 kW SOFC, 3.8 kW GT) produces power at 60% efficiency and delivers a downstream temperature of 290 °C to the recuperator. By feeding the gas stream into the absorption chiller, 8.7 kW of cooling capacity can be provided by a single-effect absorption chiller, with a COP of 0.7 and exhaust gas temperature of 104 °C. If a double effect absorption chiller is used, 14.3 kW of cooling capacity can be provided, with COP of 1.12 and exhaust gas temperature of 97 °C.

The Saito et al. [11] case operates at similar conditions to the model described here, i.e., the fuel cell current density is at 300 mA cm^{-2} and fuel utilization is 85% in both cases. The only difference is the operation temperature. The fuel cell is designed to operate at 1000 °C, with a turbine inlet temperature of 977 °C (1250 K). In the case of Saito et al. [11], both the cell and turbine inlet temperatures are 900 °C. The fluid temperature is 290 °C for Saito et al. [11], and 212 °C for this case.

In Saito et al. [11], for a SOFC-GT system producing 30 kW of electric power, a single effect absorption cooler of COP of 0.7 can provide 8.7 kW of cooling capacity. When a double effect absorption cooler with COP of 1.12 is integrated to the SOFC-GT system, 14.3 kW of cooling capacity can be provided.

Assuming that the absorption chiller has the same proportional cooling capacity performance for the 250 kW SOFC-GT system, a double effect absorption chiller can provide 119.2 kW of cooling, while 72.5 kW of cooling is available from a single effect absorption cooler.

To double check the absorption chiller cooling effect assumption based on Saito et al. [11], the performance of an off-the-shelf absorption chiller produced by BROAD, a Chinese manufacturer, has been used to compare the values [30].

The cooling water temperature is equivalent to the sea water temperature in this case. As a general rule of thumb, the sea temperature is on average 3–4 °C lower than the air (dry bulb) temperature.

5.2.3. Single effect absorption cooler

Fig. 14 shows a psychometric chart of the air conditioning process. It shows that the mixed air is cooled by the absorption chiller from station 3 to 4. From station 4 to 5, the air is cooled and water vapour is condensed at saturation using DX coil at the HVAC.

5.2.4. Double effect absorption cooler

Fig. 15 shows a psychometric chart of the air conditioning process. The shape of the air conditioning process plot is the same as that with the single effect absorption cooler. The only difference is that the position of station 4 is further away from station 3. This is because more cooling is available for a double effect absorption cooler, and the temperature drop is much more.

5.3. SOFC-GT + desiccant wheel + HVAC

The desiccant wheel removes moisture and increases dry bulb temperature, so the air needs to be cooled down by either a RTU

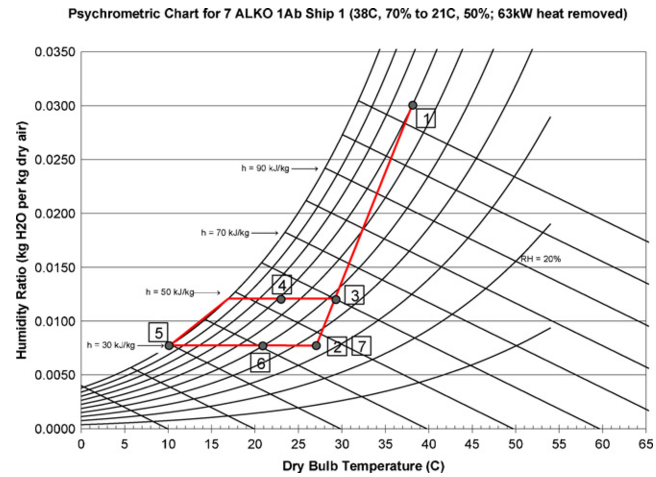

Fig. 14. Psychometric chart of SOFC-GT-single effect BROAD absorption chiller system (with 7 HVAC units) for Ship 1.

and/or an absorption cooler. A maximum temperature of 175 °C is allowed for the desiccant wheel, so the exhaust stream from the fuel cell (212 °C) needs to be cooled down.

Note that the flow rate of exhaust from the SOFC-GT system is much less compared to the HVAC air flow rate. In order for the desiccant wheel to work, the flow rates between the ventilation air and the exhaust air must be matched.

For Ship 1 using ALKO-THERM HVAC units with air flow rate of 6419 m^3 h^{-1} each, three units produces 19,257 m^3 h^{-1}. Although a desiccant wheel generally has a minimum area of a quarter for regeneration, i.e., passing hot SOFC-GT exhaust through the wheel area to remove moisture from the process stream (mixed ventilation air), the simulation software can model a minimum regeneration to process areas ratio of 0.1. With the fuel cell exhaust flow rate at 0.426 kg s^{-1}. At 175 °C, the exhaust volume flow rate is 1935 m^3 h^{-1} and this can be simulated using the desiccant software.

Assuming that the temperature is reduced to 175 °C, results from the NovelAire Technologies' desiccant wheel simulation software [32] shows that with an air flow rate of 19,257 m^3 h^{-1} (3 conventional air conditioning unit) and a regeneration air to process air ratios of 0.1, a desiccant wheel with diameter of 1525 mm and width of 200 mm can only reduce the absolute humidity from 0.01208 kg water kg^{-1} dry air to 0.01061 kg water kg^{-1} dry air, with dry bulb temperature at 58.5 °C. Further, a specific humidity of

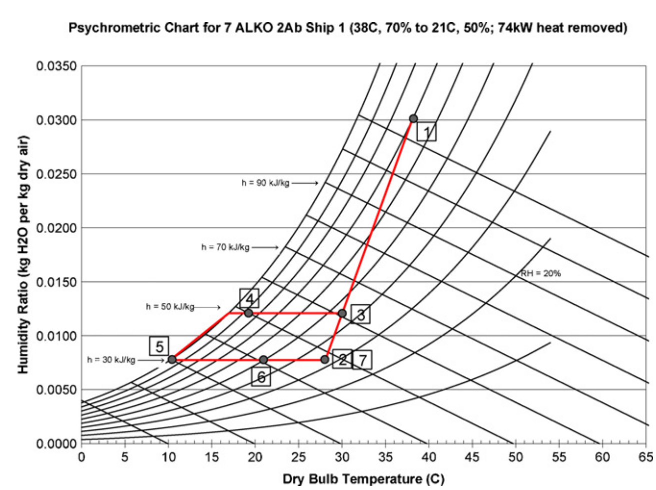

Fig. 15. Psychometric chart of SOFC-GT-double effect absorption chiller system (with 7 HVAC units) for Ship 1.

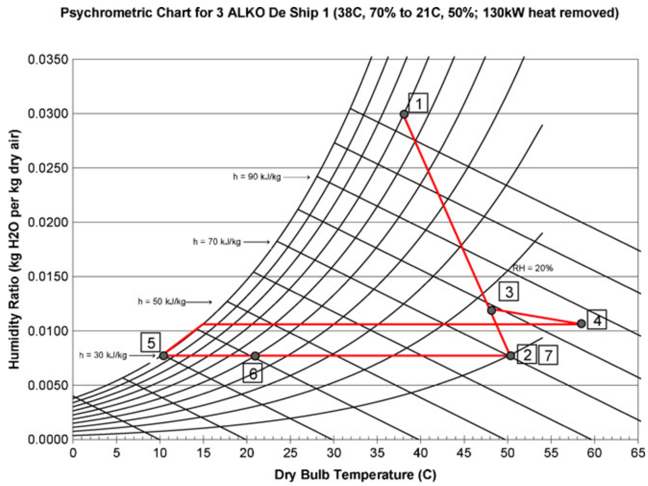

Fig. 16. Psychometric diagram for the SOFC-GT-desiccant wheel system (with 3 HVAC units) for Ship 1.

0.00773 kg kg^{-1} needs to be reached in order to achieve 21 °C of air temperature at a relative humidity of 50%.

The process sensible heat gain is 68.1 kW. After heat extraction, the exhaust temperature is 69.3 °C.

This wheel diameter is found to be the one that can dehumidify the most of the water from the incoming air. This means that the desiccant wheel cannot remove enough moisture from the outdoor air. Even if the air is cooled down by the HVAC, it needs to be cooled to condense more water before being reheated.

The advantage of using a desiccant wheel is that the waste heat from the SOFC-GT-exhaust can be utilised for drying at the desiccant wheel. The drawback is that the temperature of the dried mixed air is much higher. This means that more electricity is needed to cool down the air using the HVAC system, hence much less net electrical is left for running the ship lighting and electrical appliances.

This case shows that it is not sensible to use waste heat to dry air [using 0.034 kWe to utilise 68.1 kW heat], only to spend extra electric energy [check how much cooling and reheating needed] for cooling, reducing the electric energy available. This needs to be compared with the net electric power available, and the use of energy for cooling and reheating the single/double effect absorption chiller.

Fig. 16 shows that the air is dehumidified and heated from station 3 to 4. It is then cooled down from 58.5 °C at station 4 down to 14.9 °C, where 100% relative humidity is reached and water condenses. When the absolute humidity reaches 0.00773 kg kg^{-1} at 10.2 °C (station 5), it is then reheated to reach 21 °C at 50% relative humidity (station 6). A large reduction of specific enthalpy is required in the cooling process (from stations 4 to 5).

5.4. SOFC-GT + absorption chiller + desiccant wheel + HVAC

5.4.1. Single effect absorption chiller

If a single effect absorption cooler is used in the system, the temperature of the stream leaving the absorption cooler is 104 °C. This stream then enters a desiccant wheel for drying the incoming air (mixed with return air). Due to the relatively low temperature of the gas stream, it is calculated that a desiccant wheel with an optimal diameter of 1525 mm and width of 200 mm can only reduce the absolute humidity of the mixed air very slightly. The psychometric diagram for this system configuration is shown in Fig. 17.

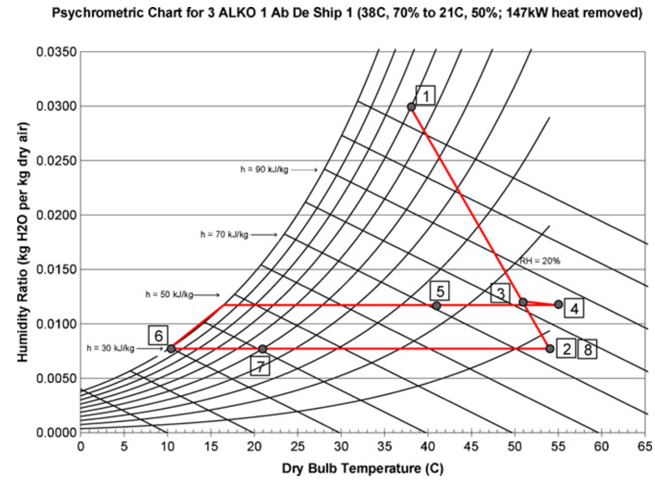

Fig. 17. Psychometric diagram for the SOFC-GT-single effect absorption chiller-desiccant wheel system (with 3 HVAC units) for Ship 1.

5.4.2. Double effect absorption chiller

If a double effect absorption cooler is used in the system, more heat energy is consumed in the air cooling process at the CHP coil than that in a single effect absorption cooler. Hence, the temperature of the stream leaving the absorption cooler is only 97 °C. This stream then enters a desiccant wheel for drying the incoming air (mixed with return air). Similar to the single effect absorption cooler scenario, it is found that a desiccant wheel with an optimal diameter of 1525 mm and width of 200 mm can only reduce the absolute humidity of the mixed air by a very small amount. The psychometric diagram for this system configuration is shown in Fig. 18.

Fig. 18 shows that the desiccant wheel only manages to reduce moisture very gently, due to the low temperature of exhaust air after passing through the double effect absorption cooler. Hence, it is a good idea to have a system configuration without any desiccant wheel for the shipping application described in this paper.

5.5. Comparison of different configurations

For configuration analysis to compare systems with desiccant wheel and/or absorption chiller, it is found that: The HVAC air flow rate for a 50 m long ship is too high compared to the exhaust gas flow rate from the SOFC-GT system. Even when the number of HVAC

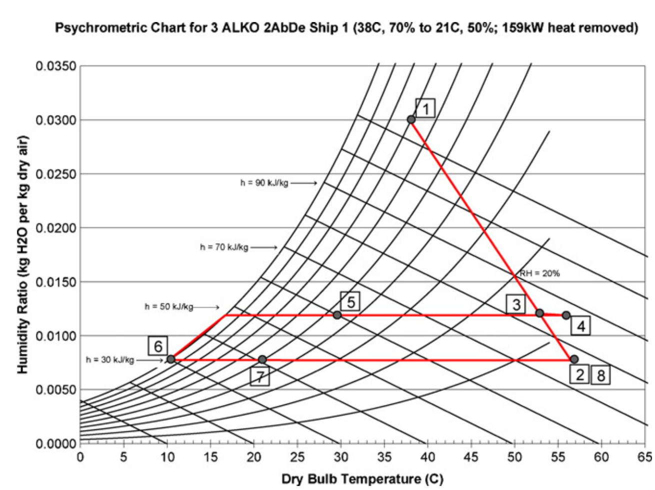

Fig. 18. Psychometric diagram for the SOFC-GT-double effect absorption chiller-desiccant wheel system (with 3 HVAC units) for Ship 1.

Table 2
Performance comparison of scenarios with desiccant wheels (and/or absorption chillers) for Ship 1 with 3 ALKO-THERM HVAC units. De, 1Ab, 2Ab in the table heading means respectively desiccant wheel, single effect absorption chiller, double effect absorption chiller.

	De	1AbDe	2AbDe	2Ab
Net electric power available for ship (kW)	130	147	159	161
Total indoor heat removal (kW)	249.5	244.9	251.8	241.7
Absorption cooling effect (kW)	0	62.4	119.2	119.2
Absorption chiller exhaust heat use (kW)	0	89.1	106.4	106.4
Desiccant wheel exhaust heat use (kW)	68.14	24.83	19.78	0
HVAC electric power with COP = 3.5 (kW)	71.29	52.14	37.88	35.01
Absorption chiller electric power (kW)	0	2.5	5	5
Desiccant wheel electric power (kW)	0.034	0.034	0.034	0
Overall system efficiency (%)	47.4	62.3	68.1	64.0

units is reduced from the typical 7 to 3, the ratio of HVAC air to exhaust is 10:1, instead of the minimum 3:1. Hence the desiccant wheel is not appropriate for this particular shipping application, and therefore not covered in the comparisons in the following sections.

The results from Table 2 show that the overall efficiency of the double effect absorption chiller-desiccant wheel-HVAC system has a higher efficiency (68.1%) than that of the double effect absorption chiller-HVAC system (64.0%) due to more exhaust heat being utilised. However, the temperature increase after the ventilation air passes through the desiccant wheel means that more electricity is needed at the HVAC to cool down air. Hence, the net electrical power available for the ship is slightly less.

In the following diagrams, the scenarios will be symbolised using the alphabets as shown in Table 3.

For configuration analysis with absorption chiller only, Scenarios a, b, c, d are compared and contrasted.

5.5.1. *Heat energy removed from the indoor environment*

Figs. 19–21 show the worst case, total heat energy that must be removed from the indoor environment for different system configurations in Ship 1 and Ship 2 respectively. The light colour section represents the amount of heat removed by absorption chiller.

In all the three Ship scenarios, Case a is the amount of energy needed to remove from the ship indoor environment, in order to achieve the required indoor temperature and humidity. It is affected by both the outdoor and indoor temperature and humidity.

Figs. 19–21 show that the worst case requires the removal of 420 kW compared with 305 kW and 295 kW respectively for Ships 1 and 2. This is due to the fact that the outdoor temperature and relative humidity for the worst case are much higher (at 45 °C and 100%), compared with Ship 1 (at 38 °C and 70%) and Ship 2 (35 °C and 85%), as listed in Table 1. At the same time, the worst case requires less condensation to reach 80% of relative humidity. Ship

Table 3
System configuration scenarios with absorption chillers.

Scenario	Absorption chiller	HVAC unit number	Returning to fresh air ratio
a	No	7	80:20
b	Saito single	7	80:20
c	BROAD single	7	80:20
d	Saito double	7	80:20

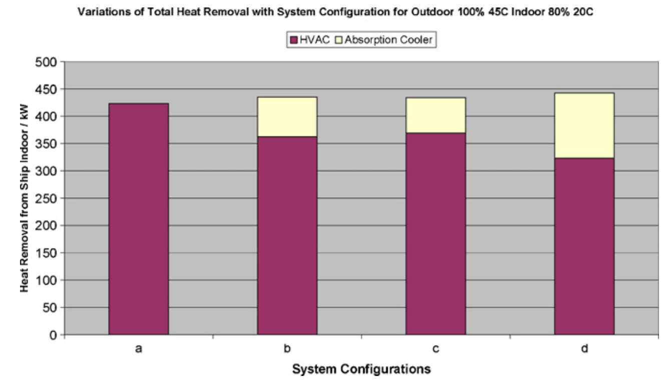

Fig. 19. Comparison of total heat energy removal required in various configurations for worst case.

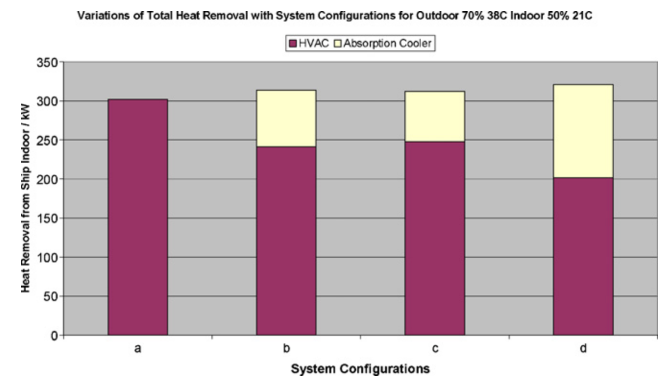

Fig. 20. Comparison of total heat energy removal required in various configurations for Ship 1.

1 requires slightly more heat energy to be removed compared with Ship 2, because more heat energy is needed to be removed to condensate water to reach the required 50% indoor relative humidity, compared to the 55% required by Ship 1. Cases b and c compare the heat removed by the absorption chiller using calculated result from Saito et al. and real performance result given at the company literature of the absorption chiller manufacturer BROAD [30]. The two results are similar. This means that the BROAD testing result has verify the accuracy of the Saito et al. model. Since BROAD has not got any double effect data sheet, the fact that the Saito single effect absorption chiller model result is shown to be reliable adds confidence to the Saito double effect absorption chiller model results, which are shown in case d in Figs. 19–21. The results shown that the double effect absorption chiller can remove 27%, 38% and 40%

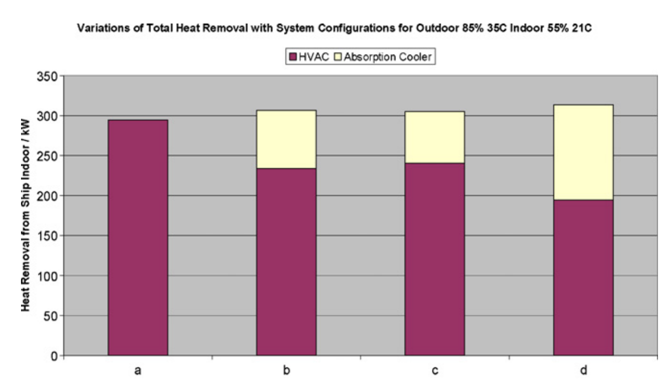

Fig. 21. Comparison of total heat energy removal required in various configurations for Ship 2.

Table 4
Net electric power of various system configurations with 7 HVAC units for three different ships.

System configurations	Net electrical power available to the ship (kW)		
	Worse case	Ship 1	Ship 2
Conventional SOFC-GT-HVAC	91.9	50.5	67.5
CCHP with Saito single effect absorption chiller	106.7	65.3	82.3
CCHP with BROAD single effect absorption chiller	104.8	63.4	80.5
CCHP with Saito double effect absorption chiller	115.5	74.1	91.1

of the total amount of heat required, for worst case, Ships 1 and 2, respectively. Hence, absoprtion cooler can save electricity required by conventional HVAC cooling.

5.5.2. Net electricity available in difference scenarios relative to SOFC-GT-conventional HVAC case

Table 4 shows that the net electrical power available for conventional system configuration (with 7 HVAC units) in the worse case, Ships 1 and 2 are, respectively: Net electricity available in difference scenarios relative to SOFC-GT-conventional HVAC case Table 4 shows that the net electrical power available for conventional system configuration (with 7 HVAC units) in the worse case, Ships 1 and 2 are, respectively: 91.9 kW, 50.5 kW and 67.5 kW. If a double effect absorption chiller is chosen, the increases in power are, respectively; 25.7%, 46.8% and 35.0% (relative to the conventional case in each ship).

It is shown that for Ships 1 and 2, the air is cooled down to a low temperature to remove moisture, and then a large amount of heat is used to reheat the air to the required temperature again. If electric heating is used, most of the energy provided by the SOFC-GT system will be consumed. One way to tackle the waste of energy could be to extract the internal heat via heat exchangers.

6. System control volume energy balance

It is useful to show the power split between parasitic losses and net electrical power available for base load. This is done to ensure energy is conserved at a system level. This also helps verify the amount of heat that must be removed from the indoor environment due to hotel load (HVAC air conditioning system, lighting, electrical appliances).

The recuperated SOFC-GT system produces 250 kW of electric power for supplying base load electrical demand (excluding propulsion) for the ship. However, not all of the electric power is used for lighting, music, entertainment and computers. Part of the energy is used for cooling, dehumidification and reheating of air in the HVAC system. The amount of energy required depends on the outdoor temperature and humidity and the indoor temperature and humidity setting. Other factors affecting the net electric power output include:

System configurations

- Conventional HVAC units
- Single/double effect absorption chiller-HVAC.

For worst case, Fig. 22 shows that most of the energy is used for HVAC cooling. This is due to the need to reduce the high temperature (45 °C) and humidity (100%) of the outdoor air. For Ships 1 and 2, as shown in Figs. 23 and 24 respectively, most of the energy is for HVAC reheating. The relative humidity that needs to be reduced by cooling plus condensing water at saturation for Ships 1 and 2 are respectively 50% and 55%, compared with 80% required in worst case.

It is worth using an absorption chiller to cool down hot ventilation air. With 2.5 kW of electric power consumption in a single effect absorption chiller, 62.4 kW of cooling (from 82.6 kW of waste heat) can be utilised for the BROAD single stage absorption cooling. This is out of the 312 kW of mixed air and indoor heat that needs to be removed for Ship 1. For a double effect absorption chiller, the use of 5 kW of electrical power makes 119.2 kW of cooling (from 106.4 kW of waste heat) available.

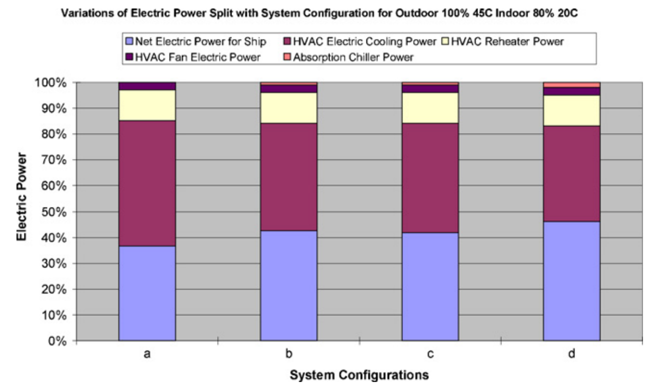

Fig. 22. Comparison of power split of 250 kW electrical power produced by SOFC-GT system in various trigeneration system configurations for worst case.

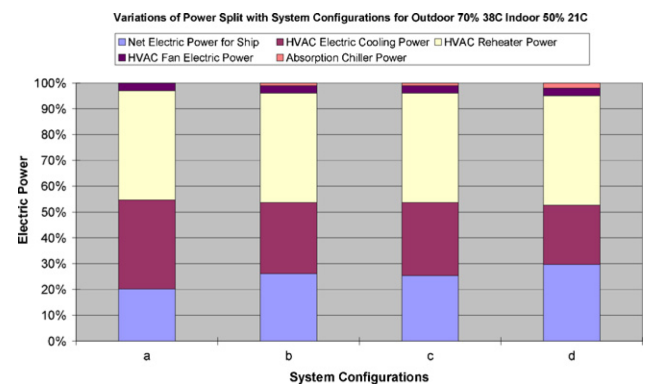

Fig. 23. Comparison of power split of 250 kW electrical power produced by SOFC-GT system in different trigeneration configurations for Ship 1.

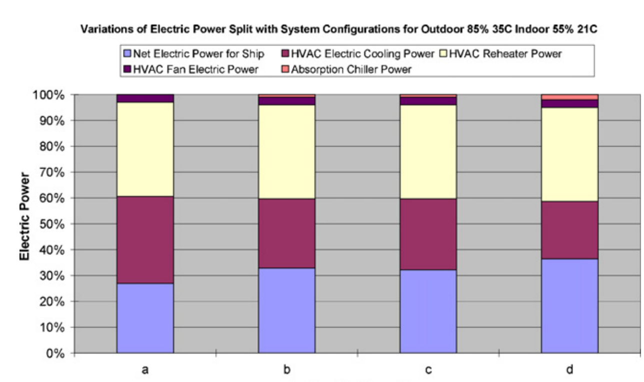

Fig. 24. Comparison of power split of 250 kW electrical power produced by SOFC-GT system in different trigeneration system configurations for Ship 2.

Table 5
The overall system efficiency of various system configurations with 7 HVAC units.

System configurations	Overall system efficiency %		
	Worse case	Ship 1	Ship 2
Conventional SOFC-GT-HVAC	22.0	12.1	16.1
CCHP with Saito single effect absorption chiller	50.3	40.4	44.4
CCHP with BROAD single effect absorption chiller	44.8	34.9	39.0
CCHP with Saito double effect absorption chiller	53.0	43.2	47.2

7. Overall system efficiency improvements by trigeneration system compared with conventional SOFC-GT system

Since waste heat from the SOFC-GT is utilised to provide some cooling via the absorption chiller, and reduce the dependency on conventional electric cooling, the efficiency of the CCHP system is increased, compared with the existing recuperated SOFC-GT system.

The overall system efficiency of different system configurations with 7 HVAC units can be summarised in Table 5. In all ships with the double effect absorption chiller in the system configuration, the efficiency is higher, due to more useful heat being used in the system.

For the worst case, the overall system efficiency improves from 22.0% for conventional HVAC units to 44.8% and 53.0% for single and double effect absorption chillers respectively. In the real case, Ship 2 is more efficient than Ship 1 by 4% for conventional, single effect and double effect absorption chiller scenarios. Due to the need to reduce humidity to a low level, water needs to be condensed to a low temperature and then the air is reheated, which consumes electricity. Hence, the reduced available net electric power leads to a lower overall efficiency.

8. Conclusions

For a 50m long ship with a 250 kW base load system, the HVAC air flow rate is too high compared to the exhaust gas flow rate from the SOFC-GT system. Even when the number of HVAC units is reduced from the typical 7 to 3, the ratio of HVAC air to exhaust is 10:1, instead of the minimum 3:1. Hence the desiccant wheel is not suitable for this particular application.

The absorption chiller makes the best use of waste heat from the SOFC-GT system. The SOFC-GT-double effect absorption chiller-HVAC system is found to be the optimum system configuration for the ship application.

The Single effect BROAD and Saito et al. results are comparable. This gives confidence that the Saito results are reliable. Also, since BROAD produces a double stage exhaust chiller for 500 °C, the data cannot be used to simulate in this case, with exhaust temperature of 212 °C. It needs to be proved that the double effect absorption chiller data from Saito et al. [11] are verified and can be used in this paper with confidence.

In all cases, the use of absorption chiller increases the net electrical power available for the ship. By using a double effect absorption chiller, more cooling is available, hence less electricity is required for conventional HVAC cooling.

For the worst case using 7 HVAC units, the overall system efficiency improves from 22.0% for conventional HVAC units to 44.8% and 53.0% for single and double effect absorption chillers respectively. In the real case, Ship 2 is more efficient than Ship 1 by 4% for conventional, single effect and double effect absorption chiller scenarios.

Acknowledgements

Many thanks to FELICITAS, the European Commission funded Sixth Framework Programme project for supporting the research featured in this paper.

References

[1] Second IMO GHG Study 2009, Update of the 2000 IMO GHG Study, Final report covering Phase 1 and Phase 2, IMO MEPC 59/INF.10, International Maritime Organisation, 2009.
[2] J. Vidal, Shipping boom fuels rising tide of global CO_2 emissions, The Guardian, United Kingdom, 2008 (13th February).
[3] J.J. Corbett, J.J. Winebreak, E.H. Green, P. Kasibhatla, V. Eyring, A. Lauer, Environ. Sci. Technol. 41 (2007) 8512–8518.
[4] J. Makower, R. Pernick, C. Wilder, Clean Edge Trends 2008, Clean Edge Inc., 2008 (March).
[5] B. Urban, Requirement specification of marine SOFC application, FELICITAS D I.1.3.1 Deliverable Report, Lürssen, 2008.
[6] International Maritime Organisation Website, MARPOL, 2008. http://www.imo.org/TCD/contents.asp?doc_id=678&topic_id=258 (accessed 09.08.10).
[7] SEAaT Website, SEAaT Sulphur Emissions Offsetting Pilot Project, 2006. http://www.seaat.org/Offsetting-Pilot-Project.aspx (accessed 09.08.10).
[8] R. Beckhaus, M. Dokupil, A. Heinzel, S. Souzani, C. Spitta, J. Power Sources 145 (2005) 639–643.
[9] S. Bensaid, S. Specchia, F. Federici, G. Saracco, V. Specchia, Int. J. Hydrogen Energy 34 (2009) 2026–2042.
[10] M. Burer, K. Tanaka, D. Favrat, K. Yamada, Energy 28 (2003) 497–518.
[11] Y. Saito, H. Yoshida, Y. Iwamoto, A. Ueda, J. Therm. Sci. Technol. 2 (2007) 168–179.
[12] G. Bizzarri, G.L. Morini, Appl. Therm. Eng. 26 (2006) 161–169.
[13] P. Colonna, S. Gabrielli, Appl. Therm. Eng. 23 (2003) 381–396.
[14] L. Lin, Y. Wang, T. Al-Shemmeri, T. Ruxton, S. Turner, S. Zeng, J. Huang, Y. He, X. Huang, Appl. Therm. Eng. 27 (2007) 576–585.
[15] X. Liao, The Development of An Air-Cooled Absorption Chiller Concept And Its Integration in CHP Systems, Doctoral Thesis, Department of Mechanical Engineering, University of Maryland, 2004.
[16] E. Cardona, A. Piacentino, Appl. Therm. Eng. 23 (2003) 1665–1680.
[17] D. Ziher, A. Poredo, Appl. Therm. Eng. 26 (2006) 680–687.
[18] E. Cardona, A. Piacentino, F. Cardona, Appl. Therm. Eng. 26 (2006) 1427–1436.
[19] E. Cardona, A. Piacentino, F. Cardona, Appl. Therm. Eng. 26 (2006) 1437–1447.
[20] H. Zhai, J.Y. Wu, R.Z. Wang, Appl. Energ. 86 (2009) 1395–1404.
[21] F. Zink, Y. Lu, L. Schaefer, Energy Convers. Manage. 48 (2007) 809–818.
[22] S. Wilkins, L.K.C. Tse, R.F. Martinez-Botas, Proc. Second European Fuel Cell Technol. Appl. Conference, EFC2007, ASME, Rome, Italy, 2007, pp. 267–268.
[23] M.G. Pangalis, R.F. Martinez-Botas, N.P. Brandon, Proc. IMechE A: J. Power Energy 216 (2002) 129–144.
[24] C. Cunnel, M.G. Pangalis, R.F. Martinez-Botas, Proc. IMechE A: J. Power Energy 216 (2002) 145–154.
[25] L. Tse, Simulation of the SOFC-GT for part-load and off-design, FELICITAS D IV.1.1.1 Deliverable Report, Imperial College, London, 2006.
[26] G. Sieros, K.D. Papailiou, Proc. 7th European conference on turbomachinery fluid dynamics and thermodynamics, Athens, Greece, 2007.
[27] Y.A. Cengel, M.A. Boles, Thermodynamics: An Engineering Approach (International Edition), fourth ed., McGraw-Hill Education, 2002, 260.
[28] S.M. Nayak, Y. Hwang, R. Radermacher, Appl. Therm. Eng. 29 (2009) 479–490.
[29] X. Liao, R. Radermacher, J. Power Sources 30 (2007) 904–911.
[30] Broad Central Air Conditioning (Absorption LiBr + H_2O) Broad X Non-Electric Chiller Model Selection and Design Manual, September 2008.
[31] H. Suzuki, M. Yamada, Y. Komoda, H. Usui, Trans. Japan Society of Refrigerating and Air Conditioning Engineers 22 (2005) 259–268.
[32] NovelAire Technologies Desiccant Dehumidification Wheel Brochure, NovelAire Technologies, 2004.
[33] T.S. Ge, Y.J. Dai, R.Z. Wang, Y. Li, Energy 33 (2008) 1807–1815.
[34] M. Kanoğlu, M.Ö. Çarpınlıoğlu, M. Yıldırım, Appl. Therm. Eng. 24 (2004) 919–932.
[35] A.A. Zadpoor, A.H. Golshan, Energy 31 (2006) 2652–2664.
[36] W. Liu, Z. Lian, R. Radermacher, Y. Yao, Energy 32 (2007) 1749–1760.
[37] H. Pundt, Requirements for thermal management of SOFC-GT systems for transport applications – evaluation of heat recovery in waterborne applications, FELICITAS DIV.1.1.1 Deliverable Report, Lürssen, 2006.
[38] L. Fu, Z.L. Zhao, S.G. Zhang, Y. Jiang, H. Li, W.W. Yang, Energy Convers. Manage. 50 (2009) 977–982.
[39] D. Stenersen, Marine Applications of Fuel Cells: User Requirements Proposal of FC Demonstration on Natural Gas Powered Ferries, Marintek, 2006.
[40] K. Mori, M. Oka, T. Ohhashi, Development of Triple-Effect Absorption Chiller-Heater, 22nd World Gas Conference Tokyo 2003 (WGC 2003), Japan, 2003.

Glossary

AHP: absorption heat pump
APU: auxiliary power unit
BIMCO: Baltic and International Maritime Council

CH_4: methane
CNG: compressed natural gas
CO_2: carbon dioxide
COP: coefficient of performance
CCHP: combined cooling heating and power
DX: direct expansion
HVAC: heating, ventilation and air conditioning
IMO: International Maritime Organisation
LNG: liquefied natural gas
LPG: liquefied petroleum gas
MARPOL: International Convention for the Prevention of Pollution from Ships
MCE: mass continuity equations
MEPC: Marine Environment Protection Committee
NOx: nitrogen oxides
PSSA: particularly sensitive sea areas
RH: reheat
RTU: roof top unit
SEAaT: shipping emissions abatement and trading
SECA: SOx emission control areas
SFEE: steady flow energy equations
SOFC-GT: solid oxide fuel cell-gas turbine
SOx: sulphur oxides
UNCLOS: United Nations Convention on the Law of the Sea